

NASA Contractor Report 3594

**A Primer on Sulfur for
the Planetary Geologist**

Eilene Theilig

**GRANT NAGW-132
SEPTEMBER 1982**

NASA



NASA Contractor Report 3594

A Primer on Sulfur for the Planetary Geologist

Eilene Theilig
Arizona State University
Tempe, Arizona

Prepared for
NASA Office of Space Science and Applications
under Grant NAGW-132



National Aeronautics
and Space Administration

**Scientific and Technical
Information Branch**

1982

TABLE OF CONTENTS

Chapter		Page
	ABSTRACT	1
1.	INTRODUCTION	1
2.	ELEMENTAL SULFUR	3
	2.1 INTRODUCTION	3
	2.2 LIQUID SULFUR	5
	2.3 SOLID SULFUR	7
3.	PROPERTIES OF ELEMENTAL SULFUR	11
	3.1 MELTING POINT AND FREEZING POINT	11
	3.2 VISCOSITY	11
	3.3 DENSITY	12
	3.4 COLOR	12
	3.5 STRENGTH CHARACTERISTICS	15
	3.6 THERMAL PROPERTIES	16
4.	SULFUR FLOWS	19
	4.1 NATURAL SULFUR FLOWS	19
	4.2 MAN-MADE SULFUR FLOWS	26
5.	SUMMARY	31
	REFERENCES	33

A PRIMER ON SULFUR

ABSTRACT

Sulfur has been proposed as the dominant composition for the volcanic material on Io. Sulfur is a complex element which forms many intramolecular and intermolecular allotropes exhibiting a variety of physical properties. Cyclo-S₈ sulfur is the most abundant and stable molecular form. The important molecular species within liquid sulfur change in concentration with temperature and consist of cyclo-S₈, polymeric chains, and small molecules as S₃, S₄, and S₅. Concentrations of the allotropes control the physical properties of the melt. Discontinuities in density, viscosity, and thermal properties reflect the polymerization process within liquid sulfur. Increasing concentrations of S₃, S₄, and S₅ with temperature cause the color change from yellow to red. Variations in the melting point are related to autodissociation of the liquid. Many solid forms of sulfur have been identified but only orthorhombic α and monoclinic β sulfur, both composed of cyclo-S₈ sulfur, are stable under terrestrial conditions. Other solid allotropes are composed of various molecular species and may be formed through reactions of sulfur compounds or by quenching the melt. Physical properties of solid sulfur are dependent on the allotrope and, in some cases, the thermal history. Although only two solid allotropes are considered stable, others may be important on Io.

Natural terrestrial sulfur flows have been identified in several areas, three of which are described here: 1) Siretoko-Iōsan, Japan; 2) Volcan Azufre, Galapagos Islands; and 3) Mauna Loa, Hawaii. All of the flows are associated with fumarolic areas and are considered to have formed by the melting and mobilization of sulfur deposits. Only the flows in Japan apparently issued from a definable vent, whereas in Volcan Azufre the flows headed in talus deposits; in Hawaii, the head of the flow was apparently covered by talus. Surface textures of the flows indicate a behavior of molten sulfur similar to that of silicate lava. Tension cracks in the top layer, pahoehoe-like surface texture, and a microcrystalline surface layer and coarsely crystalline interior all suggest the formation of a chilled crust. Channels, rivulets, and lobate edges were also described for the flows. Temperature at which sulfur was erupted was not measured for any of the flows but for various reasons none of them was considered to have erupted above 160°C.

Man-made sulfur flows may be formed as part of the Frasch mining process by which sulfur is removed from the subsurface in a liquid state. For storage purposes the molten sulfur may be pumped into large vats to solidify. As the sulfur is pumped into the vat, it forms a thin flow exhibiting smooth and irregular textures and lobate edges on both a large and small scale. Further studies of these flows could yield more information on the behavior of flowing sulfur.

1. INTRODUCTION

The Voyager 1 and 2 flybys of the jovian system revealed large plumes of material being ejected from the surface of Io through volcanic activity (Morabito *et al.*, 1979). Calderas and volcanic flows are also abundant on Io (Carr *et al.*, 1979; Smith *et al.*, 1979a). Several lines of evidence suggest sulfur as a

possible candidate (or at least an important constituent) for the volcanic material: (1) ionized sulfur has been detected in the area of Io's orbit suggesting that sulfur originates from the surface of Io; (2) spectral reflectance data for Io's surface tend to match those of various forms and compounds of sulfur

(Fanale *et al.*, 1974; Wamstecker *et al.*, 1974; Nash and Fanale, 1977; Nelson and Hapke, 1978; Fanale *et al.*, 1979); 3) color variations of red, orange, and yellow on the surface of Io can be explained by sulfur which can exhibit these colors depending on the molecular species present and the thermal history of the sulfur (Sagan, 1979); and 4) volatiles proposed to be involved in mechanisms for driving the plumes include sulfur compounds (Smith *et al.*, 1979a, b; Johnson *et al.*, 1979).

Little is known about the characteristics and behavior of molten sulfur as it is extruded as a flow and the volcanic features it may form. Silicate flows may also be present on Io (Carr *et al.*, 1979) and it is important to determine methods by which sulfur flows could be identified and distinguished from silicate flows. The behavior of sulfur is also important in considerations of volcanic processes on Io. Thus, the objective of this report is to present information on elemental sulfur which is pertinent to the study of possible sulfur flows on Io. The report is divided into three parts: 1) The first part is a discussion of solid and liquid elemental sulfur and its common forms. Several million different molecular structures for sulfur can exist; however, only a few of these are stable at standard

terrestrial conditions. Other forms may be stable under ionian conditions. 2) The second part gives known physical properties of sulfur such as melting points, viscosity, density, color, strength, and thermal properties. 3) The third section pertains to terrestrial sulfur flows, both those that occur naturally and those formed artificially in sulfur mining processes. These flows provide the only information available on characteristics of flowing sulfur.

ACKNOWLEDGMENTS..I wish to thank R. Greeley for his assistance, discussions, careful reviews, and encouragement to finish this project. I also thank B. Meyer for his clarifications and helpful suggestions. Duval Corporation provided useful information and a tour of a sulfur cooling vat for which I am grateful. Most of the figures are used with the permission of many individuals and publishing agencies. I would also like to thank those who helped put the final copy together including M. Schmelzer (typesetting), D. Ball (photography), and S. Selkirk (graphics). This work has been supported by NASA Grant NAGW 132 as part of the Jupiter Data Analysis Program of the NASA Office of Planetary Geology.

2. ELEMENTAL SULFUR

2.1 INTRODUCTION

Elemental sulfur can assume different forms exhibiting a variety of physical properties. The forms are called *allotropes* and can be divided into two types - *intramolecular allotropes*, the different molecular species resulting from chemical bonding of sulfur atoms, and *intermolecular allotropes*, the different lattice structures formed by arrangement of the molecules within crystals (Meyer, 1965). Unfortunately, a systematic nomenclature or classification of sulfur allotropes does not exist, partly because the criteria to distinguish various forms and preparations of sulfur are not consistent (Donohue and Meyer, 1965). Other complexities in understanding sulfur are: 1) most sulfur allotropes are metastable; 2) pure sulfur is difficult to obtain because it reacts readily with other substances; 3) sulfur forms many different molecular structures, several of which have similar stabilities; and 4) sulfur has a variety of similarly stable polymorphs. Designation of sulfur allotropes used in this report is given in Table 1 and will follow the nomenclature of Donohue and Meyer (1965) and Meyer (1976).

Sulfur atoms combine to form rings (cyclo-S_n) and chains (catena and polycatena sulfur), allowing several million different intramolecular sulfur allotropes to exist, if all possible combinations of the atoms are considered. Some chains or polymeric helices contain an average of 10⁶ atoms and consist of ten atoms for every three turns (Fig. 1). Theoretically, all S_n molecules with 6 < n < 12 exist as rings, and, of these, cyclo-S₈, cyclo-S₁₂, and cyclo-S₆ are the most stable, in decreasing order of stability. Molecules with more than twelve or less than six atoms can consist of either a ring or a chain configura-

tion. Larger ring structures are unstable and their formation is inhibited or interrupted by the formation of cyclo-S₈ molecules, but they do occur in sulfur liquid. The chemical difference between rings and chains is that ring molecules have fully paired electrons, whereas chains are considered to be diradicals (Meyer,

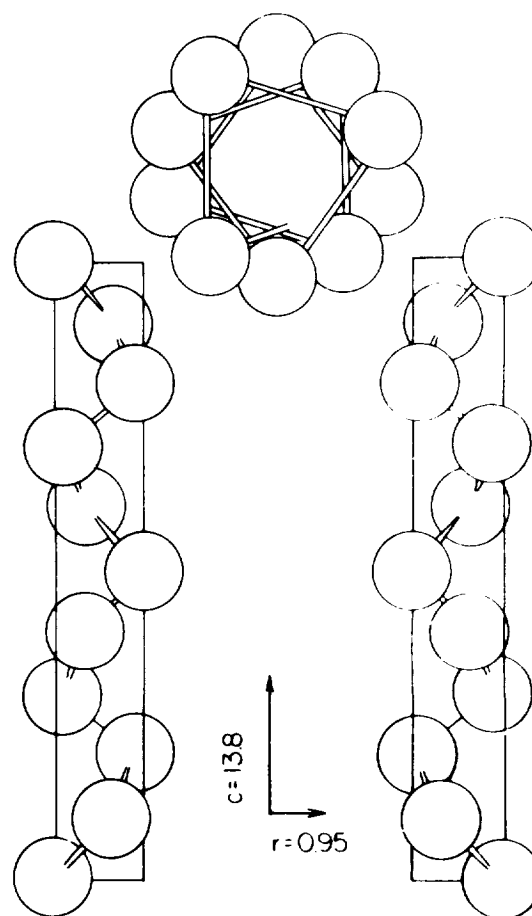


Figure 1. Helix structures of polymeric sulfur. The molecular unit consists of 10 atoms for every three turns and has an axis of $c = 13.8 \text{ \AA}$. The radius of the helix is 0.95 \AA . Left- and right-handed helices combine in various ways to form the different types of polymeric sulfur. A view down the c axis is shown at the top of the figure. (From Meyer, 1976)

Table 1. Nomenclature of Sulfur Allotropes

Name	Synonyms	Molecular species	Designation used in this review
α (alpha)	Rhombic, orthorhombic, Muthmann's I	Cycloocta-S	Orthorhombic- α
β (beta)	Monoclinic I, Muthmann's II, prismatic	Cycloocta-S	Monoclinic- β
γ (gamma)	Monoclinic II, Muthmann's III, nacreus, mother-of-pearl, Gernez	Cycloocta-S	Monoclinic- γ
δ (delta)	Monoclinic III, Muthmann's IV, γ -monoclinic	Cycloocta-S	Allotropes of S_8
ϵ (epsilon)	Engel, Aten, rhombohedral, monoclinic Engel	Cyclohexa-S	Rhombohedral
ζ (zeta)	5th monoclinic, Korinth	Cycloocta-S	Allotrope of S_8
η (eta)	4th monoclinic, Korinth	Cycloocta-S	Allotrope of S_8
θ (theta)	Tetragonal, Korinth	Cycloocta-S	Allotrope of S_8
ι (iota)	Erametsa	Cycloocta-S	Allotrope of S_8
κ (kappa)	Erametsa	Cycloocta-S	Allotrope of S_8
λ (lambda)		Cycloocta-S	Cycloocta- S_8
μ (mu)	(a) Insoluble (b) Polymeric	Catenapoly-S	Solid or liquid Polymeric-S
ν (nu)	μ	Mixture	Solid, Polymeric
ξ (xi)	Triclinic, Korinth	Cycloocta-S	Allotrope of S_8
\omicron (omicron)	Erametsa	Cycloocta-S	Allotrope of S_8
π (pi)	(a) Aten, Erametsa (b) Catenaocta-S	Ring mixture	Frozen liquid
ρ (rho)	Aten, Engel	Cyclohexa-S	Cyclohexa-S
τ (tau)	Erametsa	Cycloocta-S	Allotrope of S_8
ϕ (phi)	Fibrous	Mixture	Fibrous
φ (phi)	Fibrous, plastic	Polycatena-S	Fibrous
χ (chi)	Plastic	Mixture	Polymeric
ψ (psi)	Fibrous	Mixture	Fibrous
ω (omega)	Insoluble, white, Das supersublimation	Mixture	Polymeric
m	Triclinic	Cycloocta-S	Allotrope of S_8
n	μ		Solid, Polymeric
Aten	See ϵ , ρ	Cyclohexa-S	Rhombohedral
Braun	See μ	Mixture	Solid, Polymeric
Engel	See ϵ , ρ	Cyclohexa-S	Rhombohedral
Korinth	See ξ , η , θ , ζ	Cycloocta-S	
Muthmann	See α , β , γ , δ	Cycloocta-S	
Schmidt	See orthorhombic- S_{12}	Cyclododeca-S	
Amorphous	ω , μ	Mixture	Solid, Polymeric
Cubic	High pressure cubic plastic		High pressure forms
Fibrous	ψ , ϕ , phase II	Catenapoly-S	Fibrous
Insoluble	"Crystex," super-sublimated	Mixture	Insoluble
Laminar	Phase I, white, ω , μ , χ	Catenapoly-S	Laminar
Metallic	High pressure metallic	?	High pressure forms
Photosulfur	Insoluble	?	Photosulfur
Black	(a) Skjervan (b) Rice, Schenk	?	Quenched liquid
Brown	Maltsev	Mixture	Trapped vapor
Green	Rice	Mixture	Trapped vapor
Orange	Erametsa		
Purple	Rice	Mixture	Trapped vapor
Red	(a) Rice (b) Erametsa	Mixture	Trapped vapor
Violet	Rice	Mixture	Trapped vapor
E, F, G	Erametsa's red	Mixture	Allotrope of S_8
I, K, L, M	Orange		

Modified after Meyer, 1976.

1976). This difference is reflected by the chemical reactivity and by the physical properties. The presence and concentration of each allotrope and, therefore, the physical and chemical properties of bulk sulfur, are dependent on the thermal history of the sample. On a very broad basis, intramolecular allotropes of sulfur can be divided into four groups: 1) ring molecules with up to 20 atoms which can be isolated as solids; 2) small molecules; 3) large liquid and solid polymers; and 4) ions in solution. This report will be limited to the more common sulfur allotropes and to those which may be of particular interest for the study of Io.

2.2 LIQUID SULFUR

The equilibrium composition of liquid sulfur is dependent on temperature and consists of a complex mixture of allotropes (Fig. 2). The exact allotropic compositions have not been determined (Meyer, 1977) but molecular species which have been observed include S_2 , S_3 , S_4 , S_5 , S_6 , S_7 , S_8 , S_{12} , polycatena S_∞ (polymers) and S_π (a mixture of allotropes). The most abundant allotrope is probably cyclooctal sulfur (cyclo- S_8) which consists of a puckered ring configuration of eight sulfur atoms in which two parallel squares with atoms at the corners are rotated 45° with respect to each other (Fig. 3). This allotrope is relatively stable and also occurs in gaseous and solid states. A part of quickly quenched sulfur can be extracted with CS_2 and precipitated at $-78^\circ C$. This part of the melt is often called π -sulfur (S_π) and can be further broken down into three fractions, the first having a molecular weight of S_6 , the second containing S_8 and having an average composition of $S_{9.2}$, and a third fraction composed of large rings of S_n , $20 < n < 33$. The S_π is formed by autodissociation of the melt and determines the freezing point as will be discussed below. At about $159.4^\circ C$ the character of liquid sulfur changes as a result

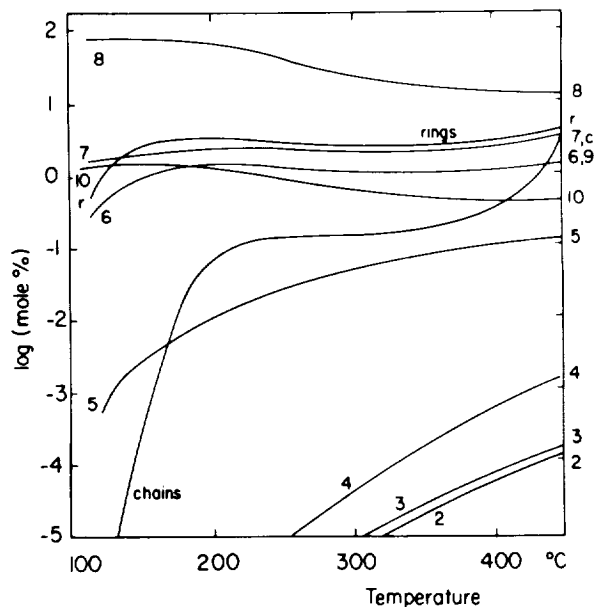
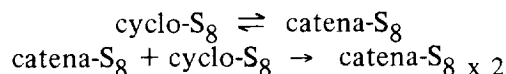


Figure 2. Estimated equilibrium composition of liquid sulfur by mole fraction. The numbers on the diagram indicate intramolecular allotropes purported to be components of liquid sulfur. Large rings (r) and chains (c) are shown as groups and not as individual allotropes. (From Meyer, 1977)

of polymerization. This temperature is commonly referred to as the λ temperature. The basic theory describing the polymerization of liquid sulfur, whereby cyclo- S_8 changes to chains or catena and polycatena, has two parts:



The first step involves the conversion of cyclo- S_8 molecules to S_8 chains which initiates polymerization. The chains propagate by the second step through which the S_8 chain combines with another cyclo- S_8 molecule which also converts to a chain structure. The chains continue to grow by adding more S_8 units (Meyer, 1976). Modifications of the theory allow for other ring structures. The average number of atoms per molecule of polycatena sulfur varies with temperature

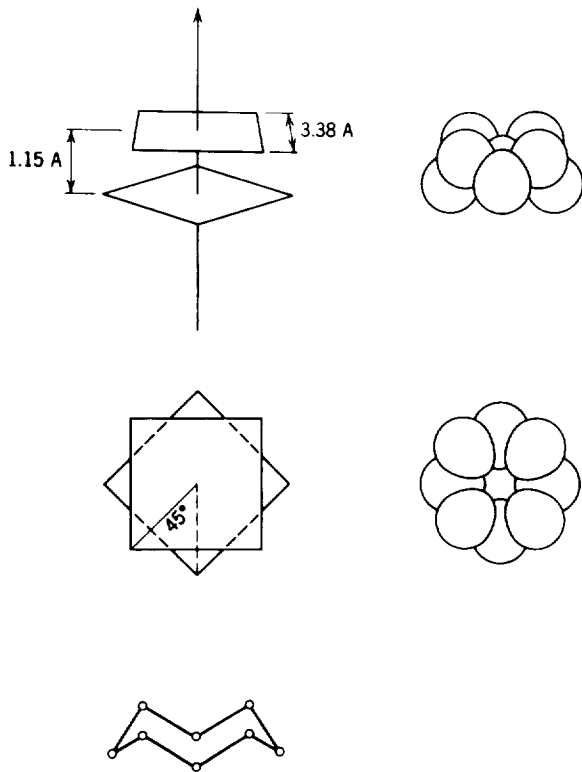


Figure 3. Structure of a cyclooctal sulfur (S_8) molecule. The atoms are located at the corners of 2 squares which are rotated 45° with respect to each other. (From Meyer, 1965)

(MacKnight and Tobolsky, 1965) as shown in Figure 4 and Table 2, with chain length reaching a maximum around 165 to 177°C. Even though the concentration of polycatena or polymer sulfur increases with temperature, above $\sim 177^\circ\text{C}$ the average chain length decreases. The equilibrium of polymerization is photosensitive and is affected by impurities such as I_2 , Cl_2 , CS_2 , H_2S , and As and by the concentration of other allotropes in the melt, such as S_6 . Spectra and other characteristics of liquid sulfur near the critical point indicate that hot liquid sulfur contains more S_2 , S_3 , and S_4 than S_5 , S_6 , S_7 , and S_8 (Meyer, 1976).

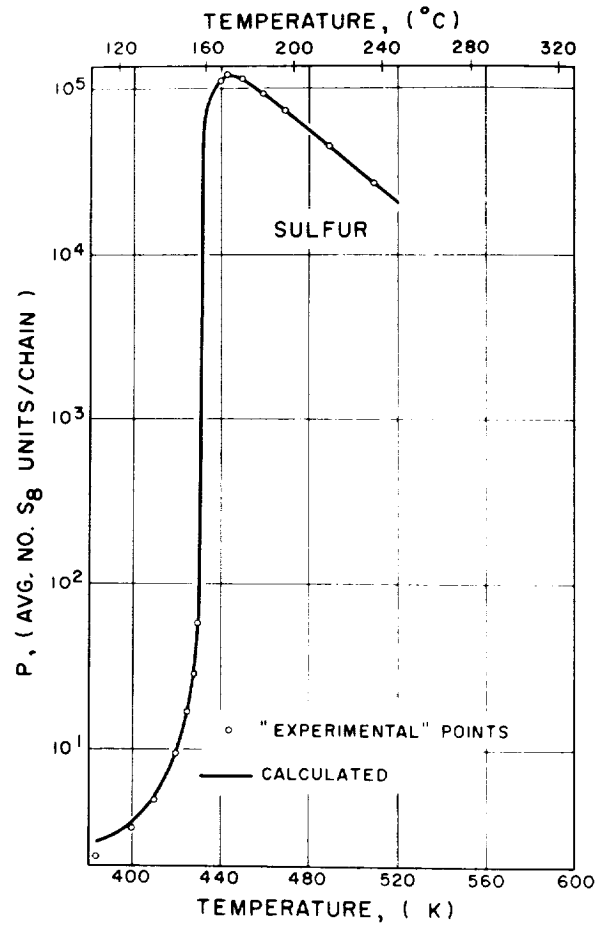


Figure 4. Average number of S_8 units per chain of polyméric sulfur versus temperature. The sharp rise at 159°C is caused by formation of chains within the liquid, whereas the decrease after 160° is caused by shortening of the chains which continue to increase in concentration. (From MacKnight and Tobolsky, 1965)

The change in molecular species within the melt is reflected by shifts in the freezing point and the discontinuities occurring in almost all physical properties at about 160°C . Establishment of dynamic equilibrium occurs slowly because of slow kinetics and can be retarded by SO_2 and acidic compounds or enhanced by ammonia and basic compounds (Tuller, 1954).

Table 2. Average Number of Catena S_8 (P) per Chain in Liquid Sulfur

Temp., K	P (in terms of S_8)
385	2.21
400	3.38
410	5.02
420	9.44
425	16.4
428	27.6
430	57.9
440	112,300
450	113,900
460	94,500
470	75,800
490	46,000
510	28,400
540	13,870
580	5,750

Modified after MacKnight and Tobolsky (1965).

2.3 SOLID SULFUR

Even though many allotropes of solid sulfur have been defined (Meyer, 1968) (Table 1), only two are thermodynamically stable, orthorhombic (α) sulfur and monoclinic (β) sulfur, both of which are composed of cyclo- S_8 molecules. The other solid allotropes are generally composed of various intramolecular allotropes and will eventually convert to a more stable form. Some of these metastable allotropes, such as cyclohexa sulfur (S_6), cyclododeca sulfur (S_{12}), and other rings, are generally formed through reactions of sulfur compounds but some have been observed in liquid sulfur. Other solid sulfur allotropes are formed by quenching the liquid sulfur and consist of polymers. Although only orthorhombic (α) and monoclinic (β) sulfur are considered stable, most of the work that has been done has not considered sulfur at 130 K, the average tempera-

ture on the surface of Io, for extended periods of time and some of the other allotropes may be stable under these conditions.

Orthorhombic sulfur, stable up to 95.3°C, is the most common form of sulfur and has been observed down to 30 K (Meyer, 1976). The unit cell is composed of 138 atoms (Donohue, 1965) (Fig. 5). The properties are not well known and this crystal form exhibits strong anisotropic effects (Meyer, 1977). Many of its properties, such as the elastic constant and thermal conductivity, are much lower along the c axis than along the a and b axes. However, in considering the properties in relation to the possible sulfur flows on Io, the anisotropic effects may not be important in a homogeneous flow with random crystal orientation. Therefore the general properties of orthorhombic sulfur should suffice for studies of Io.

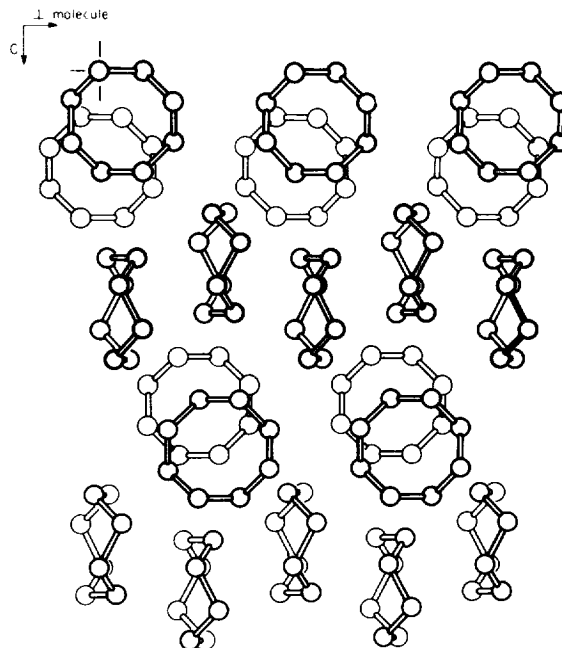


Figure 5. Part of the structure of orthorhombic (α) sulfur as viewed perpendicular to the mean plane of some of the S_8 rings. (From Donohue, 1974)

Monoclinic (β) sulfur is stable from 95.3°C to 119.6°C, its melting point. At lower temperatures monoclinic (β) sulfur will slowly transform to orthorhombic sulfur with a heat transition of 96 cal/mole; however, quenched crystals may remain monoclinic for up to a month. The structure of this allotrope (Fig. 6) is similar to that of the orthorhombic (α) except for disordered sites within the lattice where the molecules can be randomly oriented either normally or upside down. Monoclinic (β) sulfur generally forms long needles.

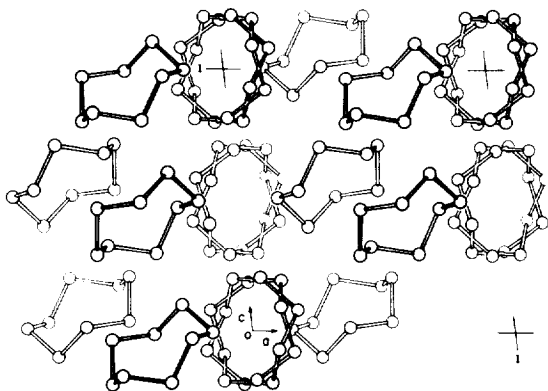


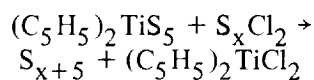
Figure 6. Structure of a unit cell of monoclinic (β) sulfur as viewed down the b axis. The sites of disordered molecules are shown by double molecules representing the orientations which the molecules may assume at random. (From Donohue, 1974)

Other allotropes which may be important on Io are solid catena and polycatena sulfur. When a sulfur melt in a nitrogen atmosphere is heated above 160°C and cooled rapidly in air, ice water, dry ice (<-78.5°C) or liquid nitrogen (between -209.86 and -195.8°C), a plastic or rubberlike material results. The sulfur is poured into the cooling medium in a thin stream and forms long fibers which can be stretched repeatedly to 10 or 15 times their original length. The ability of this material to be stretched decreases with subsequent heating of the sample until at 45°C the material can be stretched but becomes

fatigued. Various parts of this solid have been named η , μ , insoluble (polymeric) sulfur (ω), fibrous sulfur (ψ), rubbery sulfur, laminar sulfur, plastic sulfur, elastic sulfur, super-sublimation sulfur, white sulfur, and crystex. Melting curves and the temperature-pressure regions in which some of the quenched polymers are obtained are shown in Figure 7. The structure of this material is still being investigated but it apparently consists primarily of well-defined concentrations of polycatena S_{∞} arranged in helices with about 3.5 atoms per turn and other forms, dependent on its history. Of these many different forms, the molecular configuration of only fibrous and laminar sulfur is understood. Stretching during the formation of fibrous sulfur results in an almost parallel alignment of the helices, whereas the helices in laminar sulfur at least partly criss-cross. The composition of polycatena solids changes with time and conversion to orthorhombic sulfur occurs within about a month if the material is kept at room temperature. This conversion can be enhanced by mechanical stress; however, by 'working' the material the conversion is delayed. The various allotropes shown in Figure 7 are only a few which may be obtained by melting and quenching sulfur under pressure. Because of the slow kinetics and low thermal conductivity of sulfur, discussed below, dozens of different phases may exist (Meyer, 1976).

Other allotropes of solid sulfur are composed of cyclo- S_n , $6 < n < 24$. These rings are considered to occur in the equilibrium liquid near the melting point and it is possible that they may crystallize out. However, only a few of them have been formed experimentally by this method. One reason may be that these allotropes are highly metastable and quickly convert to more stable allotropes. Some of the allotropes, such as cyclo- S_6 , $-S_{10}$, $-S_{12}$, $-S_{18}$, and $-S_{20}$ can be prepared by a reaction between sulfanes and chlorosulfanes with the appropriate number of sulfur atoms and

reactive groups. Cyclo-S₇, -S₉, -S₁₀, and -S₁₁ are best prepared by:



Chemical and physical properties of these substances are incompletely known. Cyclohexa sulfur (S₆), also called rhombohedral (ρ) sulfur, forms rhombohedral crystals (Fig. 8) and decomposes in sunlight to form S₈ and S₁₂. The crystals will also decompose at 50°C and will vaporize in a vacuum. Cyclohepta sulfur (S₇) forms needles which disintegrate at 39°C. Monoclinic (γ) sulfur (S₈) will crystallize out of a melt to form needle-like crystals with 4 molecules per unit cell (Fig. 9). This form breaks down at room

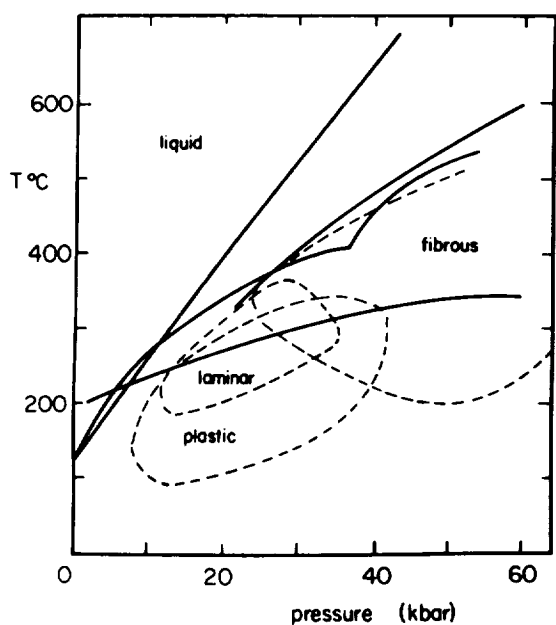


Figure 7. Pressure-temperature graph of melting curves for sulfur. The different curves represented may be the result of impurities in some of the samples tested. Slow kinetics and low thermal conductivity may be partly the cause of divergence of the melting curves since it may take days to reach equilibrium and experimenters may be observing many different phases. Zones of pressure and temperature conditions under which fibrous, laminar and plastic sulfur have been quenched are shown by dashed outlines. (From Meyer, 1976)

temperature. Twenty-four other allotropes of cyclo-S₈ have been described but they are probably mixtures of α , β , and γ sulfur. Cyclodeca sulfur (S₁₀) must be stored below -40°C and is usually produced at -78°C. Solid cyclododeca sulfur (S₁₂) is more stable than cyclo-S₆ and is formed in liquid sulfur. Each unit cell contains two molecules. Cyclooctadeca sulfur (S₁₈) forms together with cycloicosa sulfur (S₂₀), both of which consist of four molecules per unit cell. The S₁₈ is very sensitive to light and S₂₀ decomposes at 35°C but has a high melting point. Other properties of these metastable allotropes will be given below, but for further information see Meyer (1976).

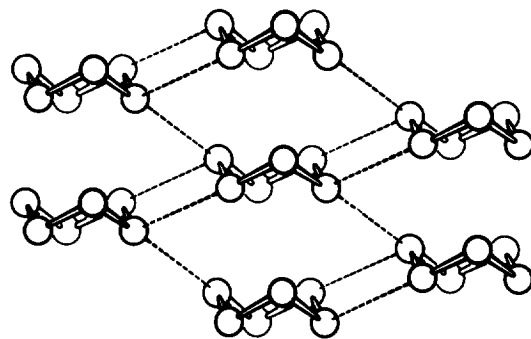


Figure 8. Structure of rhombohedral (ρ) sulfur (S₆) as viewed perpendicular to the c axis. (From Donohue, 1974)

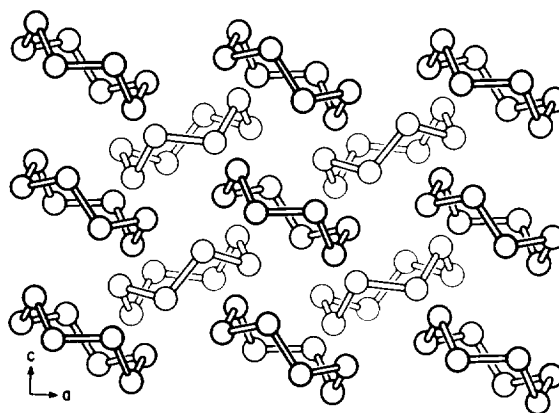


Figure 9. Structure of a unit cell of monoclinic (γ) sulfur, looking down the b axis. (From Donohue, 1974)

3. PROPERTIES OF ELEMENTAL SULFUR

3.1 MELTING POINT AND FREEZING POINT

Elemental sulfur has a variety of melting points and freezing points (Table 3) depending on the solid allotrope which is being melted and the concentrations of allotropes within the melt. Freezing point depression will occur naturally as a result of autodissociation of the melt to form S_n which has a lower freezing point than cyclo- S_8 . Therefore, the freezing point of the whole mixture is lowered accordingly. The temperature at which the maximum concentration of S_n is reached will be the lowest freezing point and is called the 'natural' melting point. The freezing point is also influenced by the pressure and temperature of the melt indicating slow kinetics and complexities within the liquid as it is cooled. Different reaction paths are followed as sulfur cools, which result in different metastable mixtures of different metastable allotropes, probably mostly rings (Meyer, 1976).

Single crystals of monoclinic (β) sulfur melt at 119.6°C and are in equilibrium with a liquid of unknown composition. The 'natural' melting point is 114.6°C and calculations indicate that the 'ideal' melting point may be as high as 133°C. Single crystals of orthorhombic (α) sulfur do not readily convert to monoclinic (β) sulfur but tend to melt at 112.8°C. The freezing point depression of orthorhombic sulfur produces a 'natural' melting point of 110.06°C (Tuller, 1954). Microcrystals of both common stable allotropes have higher melting points than larger crystals (Thackray, 1970) such that microcrystals of monoclinic (β) melt at 120.4°C and orthorhombic (α) microcrystals melt at 115.11°C. Melting points of other solid allotropes are given in Table 3. Small

droplets, diameter about 0.2 μ , can be supercooled to about 25°C for up to 20 days before crystallization occurs.

Table 3. Melting Points of Sulfur

Allotrope	Mp, °C	Remarks
alpha-S	110.06	'Natural'
	112.8	Single crystal
	115.11	Microcrystal
beta-S	114.5	'Natural'
	119.6 ^a	'Ideal' and obsd
	120.4	Microcrystal
	133	'Ideal' calcd
gamma-S	106.8	Classic
	108	Optical, DTA
	108.6	Microcrystal
insoluble-S	77; 90; 160	Optical, TDA, DTA
	104	
S_n	75	Optical
	104	Classic
S_6	(50-)	Decomposition
S_{12}	148	Decomposition
S_{18}	128	Decomposition
S_{20}	124	Decomposition

a) Thermodynamic melting point.
Modified after Meyer (1977).

3.2 VISCOSITY

The viscosity of liquid sulfur decreases with increasing temperature to about 7 centipoise at 160°C, at which point the viscosity increases rapidly to a maximum of about 932 poise at around 190°C (Fig. 10 and Table 4). With increasing temperature, the viscosity again decreases. The change in viscosity is related to the concentration and length of polycatena S_∞ within the liquid (Fig. 4). The jump in viscosity at around 160°C reflects the increase in both the concentration and the length of polycatena molecules, whereas the decrease with in-

creasing temperature after $\sim 190^\circ\text{C}$ reflects the general decrease in the number of S_8 chains per polycatena molecule. Original viscosity measurements were made by Bacon and Fanelli (1943).

At temperatures close to the melting point and at high temperatures ($>250^\circ\text{C}$), sulfur is much less viscous than most terrestrial lavas. Viscosity of an olivine basalt flow at Gembudo, Japan ranged from 137 poise at 1400°C to 37,900 poise at 1150°C ; less viscous flows include a tachylite at Mauna Iki, Hawaii that ranged from 76 poise at 1314°C to 4950 poise at 1074°C and a nepheline basalt in Japan that ranged from 80 poise at 1400°C to 190 poise at 1200°C (Clark, 1966). Viscosity values for lunar basalts are typically an order of magnitude less than those for terrestrial lavas (Murase and McBirney, 1970). Only when the sulfur is above 300°C or ~ 160 to 190°C would it have viscosities comparable to lunar lavas.

3.3 DENSITY

Meyer (1976) gives the densities of many solid sulfur allotropes as shown in Table 5. The density of liquid sulfur decreases with increasing temperature as shown in Table 6 and Figure 11. Polymerization of the melt produces a discontinuity in the density curve at the λ temperature. This break is illustrated in Figure 12.

3.4 COLOR

The color of the various sulfur allotropes and of sulfur melt, which may retain its color upon quenching, are very important for the study of possible sulfur flows on Io. Unfortunately, the color of elemental sulfur is as complex as the chemistry. For solid ring allotropes, the colors are well established (Table 7). Pure liquid sulfur is bright, clear yellow at the melting point and consistently changes to deep, opaque red, which is reached

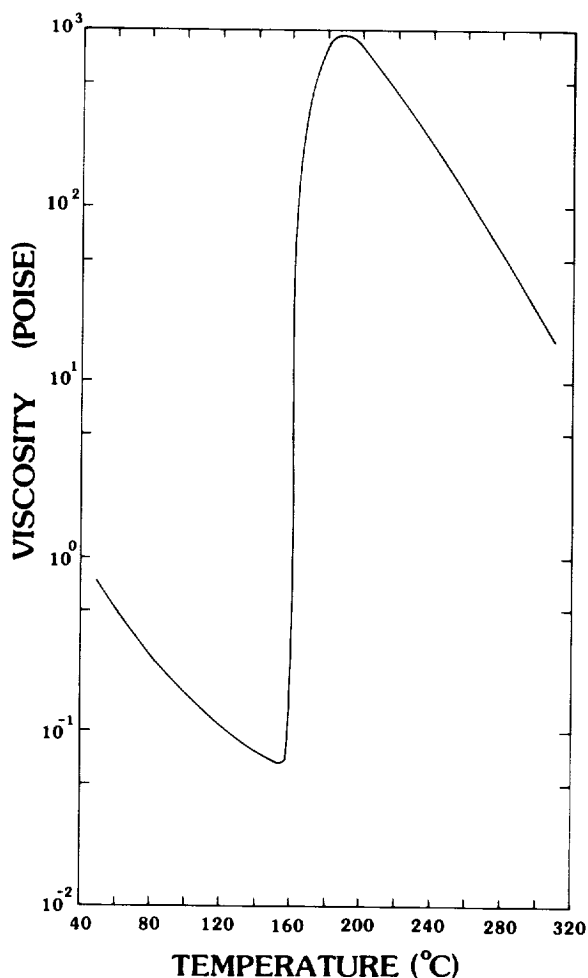


Figure 10. Viscosity curve of liquid sulfur related to temperature. Polymerization of the melt to form long chains causes the increase in viscosity around 160°C . The decrease in viscosity at higher temperatures is the result of a decrease in average chain lengths. Viscosity is displayed on a log scale of poise. Data used to graph the curve are shown in Table 4.

at the boiling point, 444°C . Dependence of the color on temperature results from the changing chemistry of the melt such that the yellow from the melting point to above 250°C is due to thermal broadening of the cyclo- S_8 spectrum and overlap of the polymeric sulfur spectrum and the red is due to the absorption spectra of S_3 , S_4 , and S_5 (Meyer *et al.*, 1971 and Meyer, 1976). The usually observed change to brown and then

Table 4. Viscosity of Liquid Sulfur

Temperature		Viscosity		State
°C	°F	poise	lb/ft. sec	
48.9	120	0.759	0.051	Supercooled liquid
60.0	140	0.491	0.033	Supercooled liquid
71.1	160	0.342	0.023	Supercooled liquid
82.2	180	0.253	0.017	Supercooled liquid
93.3	200	0.193	0.013	Supercooled liquid
104.4	220	0.149	0.010	Supercooled liquid
115.6	240	0.119	0.008	Normal liquid
121.1	250	0.110	0.0074	Normal liquid
126.7	260	0.100	0.0067	Normal liquid
132.2	270	0.090	0.0060	Normal liquid
137.8	280	0.080	0.0054	Normal liquid
143.3	290	0.074	0.0050	Normal liquid
148.9	300	0.070	0.0045	Normal liquid
154.4	310	0.066	0.0044	Normal liquid
157.2	315	0.067	0.0045	Normal liquid
158.9	318	0.119	0.008	Normal liquid
162.8	325	119.1	8.00	Normal liquid
165.6	330	208.3	14.0	Normal liquid
171.1	340	461.3	31.0	Normal liquid
182.2	360	892.9	60.0	Normal liquid
187.8	370	931.6	62.6	Normal liquid
193.3	380	907.8	61.0	Normal liquid
198.9	390	818.5	55.0	Normal liquid
204.4	400	729.2	49.0	Normal liquid
215.6	420	565.5	38.0	Normal liquid
226.7	440	386.9	26.0	Normal liquid
237.8	460	245.5	16.5	Normal liquid
248.9	480	163.7	11.0	Normal liquid
260.0	500	111.6	7.5	Normal liquid
271.1	520	74.4	5.0	Normal liquid
282.2	540	52.1	3.5	Normal liquid
293.3	560	34.2	2.3	Normal liquid
304.4	580	22.3	1.5	Normal liquid
315.5	600	17.8	1.2	Normal liquid

Modified after Tuller (1954).

Table 5. Density of Solid Sulfur Allotropes

Allotrope	Symbol	Density g/cm ³
orthorhombic α	S ₈	2.069
monoclinic β	S ₈	1.940
monoclinic γ	S ₈	2.19
cyclohexa	S ₆	2.209
cyclohepta	S ₇	2.090
cyclododeca	S ₁₂	2.036
cyclooctadeca	S ₁₈	2.090
cycloicososa	S ₂₀	2.016
fibrous	S _{∞}	2.010

(Meyer, 1976).

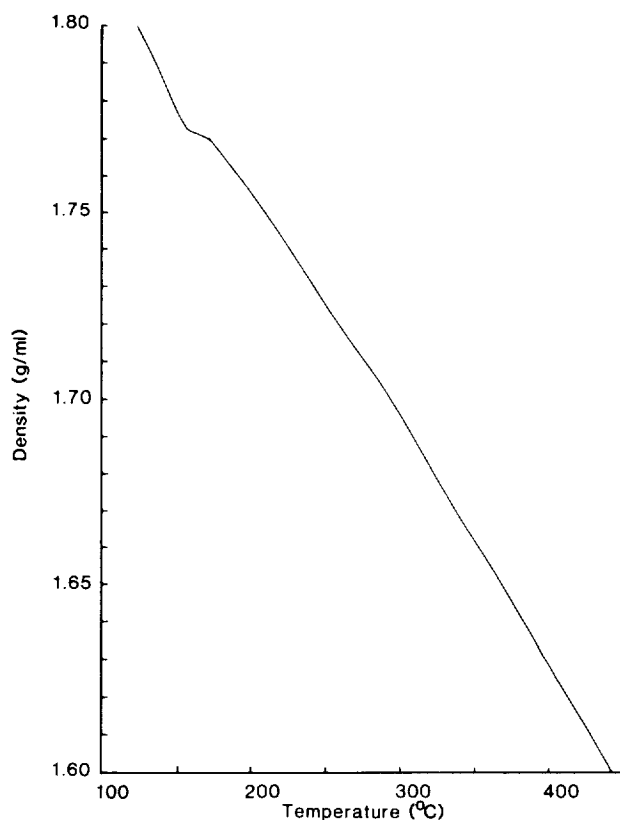


Figure 11. Density curve of liquid sulfur. A slight discontinuity at the λ temperature is represented by a change in slope around 160°C. Derived from data in Table 6.

Table 6. Density of Liquid Sulfur

°C	°F	g/ml	lb/ft ³
121.1	250	1.8037	112.60
123.9	255	1.8007	112.41
126.7	260	1.7981	112.25
129.4	265	1.7957	112.10
132.2	270	1.7935	111.96
135.0	275	1.7912	111.82
137.8	280	1.7888	111.67
140.6	285	1.7864	111.52
143.3	290	1.7842	111.38
146.1	295	1.7818	111.23
148.9	300	1.7795	111.09
151.7	305	1.7773	110.95
154.4	310	1.7752	110.82
156.9	314	1.7739	110.74
158.5	317	1.7729	110.67
161.0	322	1.7723	110.64
165.0	329	1.7714	110.60
171.3	340	1.7705	110.53
178.3	353	1.7671	110.31
184.0	363	1.7644	110.14
210.0	410	1.7509	109.30
239.5	463	1.7329	108.18
278.5	533	1.7096	106.72
357.0	675	1.6583	103.52
445.0	833	1.6060	100.26

Modified after Tuller (1954).

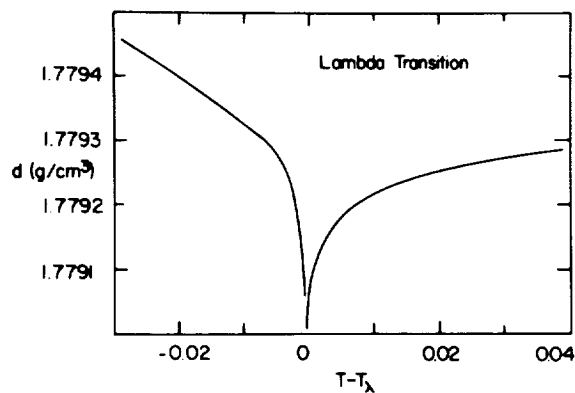


Figure 12. Discontinuity of the density of liquid sulfur in the narrow range around the λ temperature of 159.4°C. This is the point of polymerization in the melt. (From Meyer, 1976)

black as the temperature increases is not observed in very pure sulfur (99.99+% sulfur). At high temperatures sulfur is very reactive and the darkening of the fluid to brown and black is considered to be a result of a reaction with impurities, possibly organic (Meyer, 1976).

The color of the quenched solid is dependent on rate of cooling. If the melt is quenched from near the boiling point to -80°C , the solid will be yellow, whereas if it is quenched in liquid nitrogen (~ 209 to -196°C) a red glass will be produced. This glass will convert to yellow polymeric sulfur at -80°C (~ 193 K). Slow kinetics and low conductivity of sulfur allow only a thin film of material to be quenched, and even as the cooling occurs, chemical changes take place within the melt.

Quenching of at least the surface of sulfur flows on Io might be expected since the surface temperature is about 130 K. This falls within the temperature range of quenched yellow sulfur (-80°C or 193 K) and

Table 7. Color of Solid Allotropes

Allotrope	Symbol	Color
cyclohexa	S ₆	orange-red
cyclohepta	S ₇	light yellow
orthorhombic <i>a</i>	S ₈	bright yellow
monoclinic β	S ₈	yellow
monoclinic γ	S ₈	light yellow
cycloennea	S ₉	deep yellow
cyclodeca	S ₁₀	yellow-green
cyclooctadeca	S ₁₈	lemon yellow
cycloicosa	S ₂₀	pale yellow

(Meyer, 1976).

red sulfur (~ 78 K). Because the surface temperature is below the conversion point of -80°C , red may be the more prominent color; however, more work is needed to determine exactly what color(s) may be expected and the stability of the solid under ionian conditions.

3.5 STRENGTH CHARACTERISTICS

Dale and Ludwig (1965) review tensile and compressive strength values for sulfur and provide a more comprehensive determination of tensile strengths. Strength of sulfur is determined by the purity and thermal history of the sample. Compressive strengths of sulfur vary from 12,410.6 kPa (1800 psi) to 22,752.7 kPa (3300 psi); however, the purity and thermal history of these samples were not discussed. Tensile strengths were determined for a large range of thermal histories and it appears that rate of cooling and the temperature to which the sample was heated are important. A faster rate of cooling and a higher initial temperature of the melt result in higher tensile strengths. Monoclinic (β) sulfur heated to 130°C possessed tensile strengths of 399.9 kPa (58 psi) to 441.3 kPa (64 psi), whereas monoclinic sulfur produced from a melt at 187°C possessed tensile strengths from 427.5 kPa (62 psi) to 1,792.6 kPa (260 psi). Orthorhombic (*a*) sulfur from a melt at 130°C had tensile strengths from 330.9 kPa (48 psi) to 3,344.0 kPa (485 psi) and that from 187°C had tensile strengths ranging from 337.8 kPa (49 psi) to 4,274.7 kPa (620 psi). The samples used by Dale and Ludwig (1965) in determining tensile strengths contained minor amounts of carbon, hydrocarbon, acid, and ash so they may not represent strengths of pure sulfur. Threads of polymeric sulfur had tensile strengths from 17,926.4 kPa (2600 psi) to greater than 96,526.6 kPa (14,000 psi).

3.6 THERMAL PROPERTIES

Thermal properties of sulfur also exhibit discontinuities caused by polymerization. Thermal conductivity is greater in solid sulfur than liquid (Tuller, 1954) as shown in Table 8 and Figure 13. The thermal conductivity of sulfur is about an order of magnitude less than that of most rocks and is comparable to such insulation materials as mica and asbestos. Specific heat values for solid and liquid sulfur, at atmospheric pressure, as a function of temperature are shown in Table 9 (Tuller, 1954). Figure 14 illustrates the difference in specific heat between orthorhombic (α) and monoclinic (β) sulfur and the discontinuity in the melt at 160°C. The coefficient of thermal expansion for sulfur reaches a maximum around 152°C and rapidly decreases around 160°C (Table 10). A second maximum occurs around 288°C (Tuller, 1954). Thermal expansion of fibrous sulfur is 94×10^{-6} cm/deg for the a-axis and 72×10^{-6} cm/deg for the b-axis (Meyer, 1976).

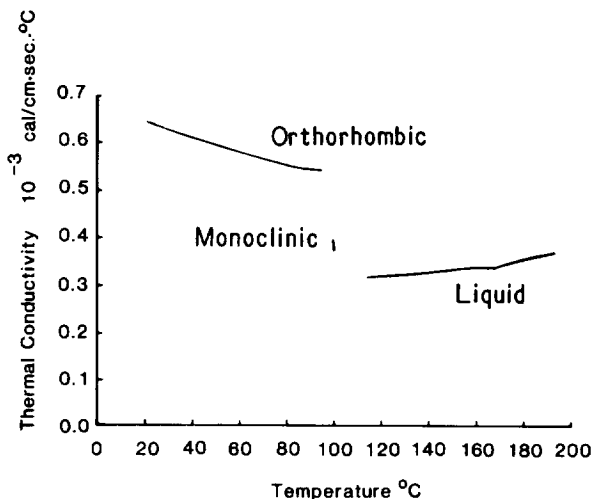


Figure 13. Thermal conductivity curves of orthorhombic (α), monoclinic (β), and liquid sulfur as derived from data in Table 8.

Table 8. Thermal Conductivity

Temperature °F	Temperature °C	Thermal Conductivity		State
		Btu/(ft)(hr)(°F)	10^{-3} cal/(cm)(sec)(°C)	
70	21.11	0.157	0.643	Orthorhombic α aggregate
100	37.78	0.149	0.616	"
120	48.89	0.145	0.600	"
140	60.11	0.141	0.583	"
160	71.11	0.137	0.567	"
180	82.22	0.134	0.554	"
200	93.33	0.133	0.550	"
203	95.00	0.132	0.546	"
212	100.00	0.090 - 0.096	0.372 - 0.397	Monoclinic β aggregate
239	115.00	0.076	0.314	Liquid
260	126.67	0.077	0.318	"
280	137.78	0.078	0.323	"
300	148.89	0.079	0.327	"
320	160.00	0.081	0.335	"
329	165.00	0.081	0.335	"
340	171.11	0.083	0.343	"
360	182.22	0.085	0.352	"
380	193.33	0.088	0.364	"

Modified after Tuller (1954).

Table 9. Specific Heat of Sulfur

SOLID				LIQUID		
Temperature		Orthorhombic (α) cal/gK	Monoclinic (β) cal/gK	Temperature		cal/gK
$^{\circ}\text{F}$	$^{\circ}\text{C}$			$^{\circ}\text{F}$	$^{\circ}\text{C}$	
-420	-267.8	0.0220		238.1	114.5	0.238
-400	-240.0	0.0365		250	121.1	0.240
-350	-212.2	0.066	0.066	270	132.2	0.244
-300	-184.4	0.088	0.088	290	143.3	0.250
-250	-156.7	0.105	0.107	300	148.9	0.256
-150	-101.1	0.134	0.138	310	154.4	0.274
-100	-73.3	0.145	0.150	315	157.2	0.300
-50	-45.6	0.153	0.159	316.5	158.1	0.445
0	-17.8	0.160	0.166	318	158.9	0.400
20	-6.7	0.162	0.169	320	160.0	0.364
30	-1.1	0.163	0.171	325	162.8	0.335
40	4.4	0.164	0.172	330	165.6	0.319
60	15.6	0.167	0.173	340	171.1	0.330
80	26.7	0.169	0.177	350	176.7	0.287
100	37.8	0.171	0.179	370	187.8	0.274
120	48.9	0.173	0.181	400	204.4	0.266
140	60.0	0.175	0.184	440	226.67	0.260
160	71.1	0.177	0.186	470	243.3	0.258
180	82.2	0.180	0.188	510	265.6	0.260
200	93.3	0.1817	0.1908	550	287.8	0.262
215.7	102.1		0.1923	600	315.6	0.266
217.5	103.1		0.1926	700	371.1	0.276
				800	426.7	0.283

Modified after Tuller (1954).

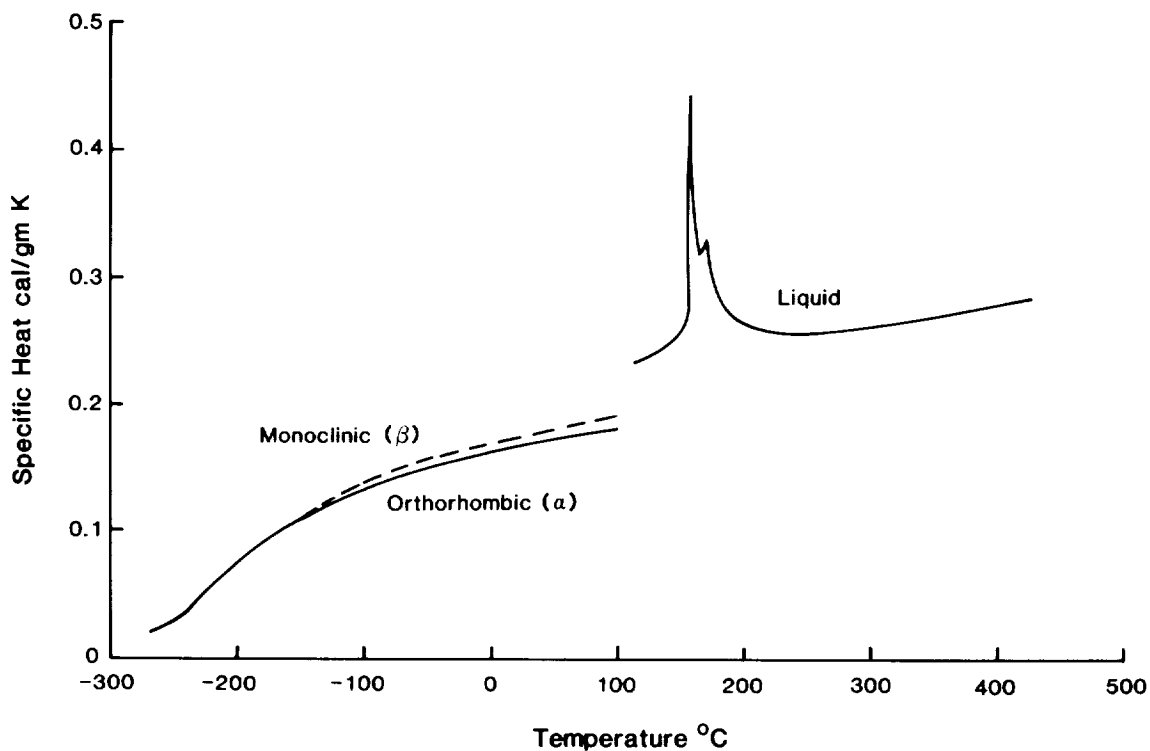


Figure 14. Specific heat of solid and liquid sulfur. Data for the curves are shown in Table 9.

Table 10. Thermal Expansion of Liquid Sulfur

Temperature		Fractional cubic expansion per °F	Temperature		Fractional cubic expansion per °F
°C	°F		°C	°F	
121.1	250	237×10^{-6}	190.6	375	168×10^{-6}
148.9	300	270×10^{-6}	204.4	400	176×10^{-6}
151.7	305	274×10^{-6}	232.2	450	196×10^{-6}
154.4	310	273×10^{-6}	260.0	500	203×10^{-6}
157.2	315	160×10^{-6}	287.8	550	204×10^{-6}
162.8	325	70×10^{-6}	315.6	600	203×10^{-6}
171.1	340	100×10^{-6}	371.1	700	195×10^{-6}
176.7	350	130×10^{-6}	398.9	750	188×10^{-6}

Modified after Tuller (1954).

4. SULFUR FLOWS

4.1 NATURAL SULFUR FLOWS

Introduction

Natural sulfur flows are rare on the Earth but are known to occur in some basaltic and andesitic volcanic areas in association with fumaroles. Three areas where natural sulfur flows have been identified are Siretoko-Iōsan, Japan; Sierra Negra caldera, Galapagos Islands; and Mauna Loa, Hawaii.

The only observation of molten sulfur eruptions was by Watanabe (1940) in 1936 at Siretoko-Iōsan volcano in Hokkaidō, Japan (Fig. 15). This andesitic volcano is part of the Kurile volcanic zone and forms the central part of a peninsula extending into the Okhotsh Sea. Historic sulfur eruptions have originated from Sulphur Crater, a horseshoe-shaped parasitic explosion crater on the western side of the volcano. The eruptions were generally a cyclic combination of steam explosions with intermittent effusion of

sulfur and hot water. Sulfur from the crater flowed down a tributary valley then followed the main valley of the Kamuiwakka River (Fig. 16). In 1889, an eruption yielded approximately 80,000 tons of relatively pure sulfur which was almost completely removed by mining prior to the next eruption. Another eruption of Sulphur Crater in 1936 lasted several months and included 40 individual sulfur flows. The liquid sulfur flowed downslope about 1400 m with an elevation drop of 400 m and reached maximum widths of 20 to 25 m near the distal ends of the flows. Total thickness of the flows varies and in some places is over 5 m. This area has long been known as a source of sulfur, and other eruptions may have occurred but were not recorded.

Sulfur flows on Isabela Island in the Galapagos Islands were first reported by Banfield (1954). Further investigation by Colony and Nordlie (1973) indicates that sulfur flows are a recurring phenomenon at Volcan Azufre,



Figure 15. Sulfur flows from Sulphur Crater (c) on the western slope of Siretoko-Iōsan volcano, Japan. Sulfur erupted from the explosion crater in 1936 and flowed about 1400 m. The scale for this photograph is provided by men (m) crossing the light colored sulfur flows (s). (From Watanabe, 1940)

a site of current fumarolic activity and sulfur deposition in the Sierra Negra caldera. The fumaroles have been localized by a fault which forms the western, talus-covered scarp of a sinuous ridge extending across the western part of the caldera floor (Fig. 17). Much of the surface is covered by sulfur deposits and individual gas vents are marked

by sulfur cones averaging 0.5 m in height. The sulfur flows are located downslope from the fumaroles and average 5 to 10 m long and a few centimeters thick. The largest flow, however, is 225 m long, 30 m wide at the distal end, and 0.5 m to a few centimeters thick, with thickness decreasing downslope. Although flowing sulfur was not observed at

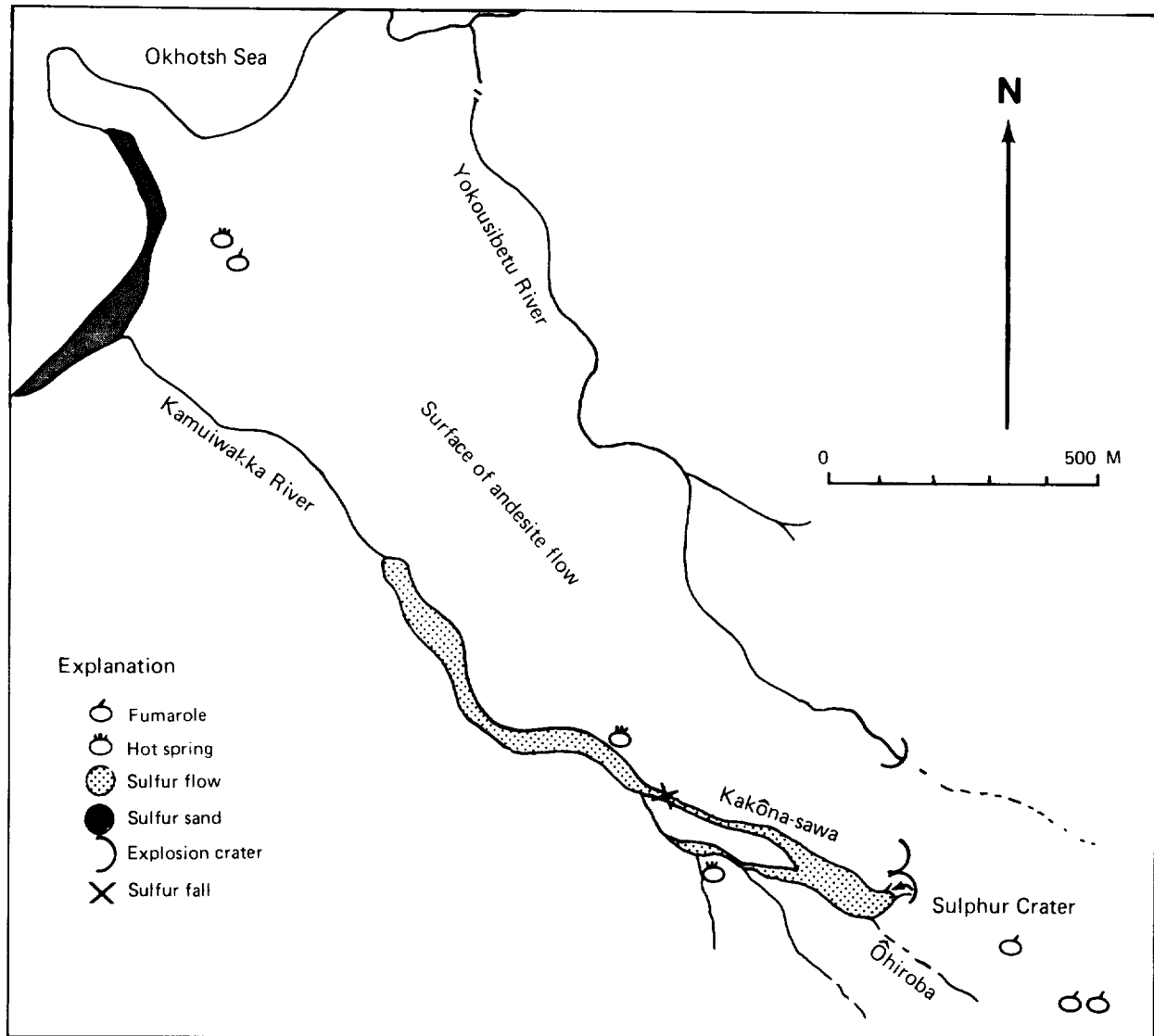


Figure 16. Map of part of the western flank of Siretoko-Iōsan volcano showing the location and distribution of the sulfur flows from Sulphur Crater. Forty individual flows were erupted in 1936. Sulfur sand formed along the beach of the Okhotsh Sea as it was eroded by the Kamuiwakka River. A sulfur fall formed by sulfur flowing over a steep cliff at the junction of the Kakōna-sawa and Kamuiwakka valleys. Locations of hot springs, fumaroles, and explosion craters are also shown. (After Watanabe, 1940)



Figure 17. Fumaroles at Volcan Azufre on Isabela Island, Galapagos. Fumarolic activity is controlled by a fault forming the western slope of a sinuous ridge, in the right foreground, which crosses the western side of the Sierra Negra caldera. The western rim of the caldera is in the left background. Sulfur flows are associated with the fumaroles. (From Colony and Nordlie, 1973)

Volcan Azufre, stratigraphy of the flows and the various states of degradation suggest that the formation of sulfur flows is an ongoing process (Colony and Nordlie, 1973).

A single sulfur flow associated with a pyroclastic cone on the southwest rift of Mauna Loa has been identified by Skinner (1970). The flow extends downslope from the lower part of Sulphur Cone and is truncated by a graben formed during the 1950 eruption of Mauna Loa. Only minimum dimensions of 27 m long, 14 m wide, and 10 to 45 cm thick can be established for the flow since the distal end is truncated and the source vent is covered by talus. When the area was first surveyed in 1921 sulfur deposits covered the area but no flow was recorded. Therefore this sulfur flow may have occurred sometime between 1921 and 1950.

Vents

The vents for sulfur flows at Volcan Azufre vary greatly from those at Siretoko-Iôsan. At Volcan Azufre, the flows appear to head in the fumarolic sulfur deposits or from the talus slope and no specific vents could be identified. Small pockets of liquid sulfur were present within and near some of the sulfur cones, but none of the flows was associated with these pockets. Occasionally part of the sulfur cones would break off and fall into the vent, resulting in remelting of the sulfur which was then ejected as spatter. Skinner (1970) states that the upper end of the sulfur flow on Mauna Loa begins about one-third of the way up the slope of Sulphur Cone, but has been covered by talus. However it is possible that, like the flows in the Galapagos, this

flow also heads in the surface material and did not have a specific opening from which it erupted.

In contrast to the flows in the Galapagos Islands and Hawaii, the sulfur flows in Japan erupted from two well-defined vents within Sulphur Crater. This explosion crater is about 30 m in diameter and was filled in 1936 with sulfur deposits and andesitic blocks. During the earlier period of eruption sulfur flowed from a funnel-shaped hole in the floor of the crater. As the activity progressed a second smaller hole was formed through which the later sulfur was erupted. This second hole was tunnel-shaped. After being erupted the sulfur flowed out through the break in the wall of the crater (Fig. 18).

Temperature of Eruption

The temperature of erupted sulfur has never been measured at a vent. Watanabe (1940) obtained the temperature of 118° to 120°C for the sulfur downslope from the vent; however, he considered the temperature at the vent to be higher, possibly between 130° to 160°C, based on experimental data, viscosity (very fluid), color (chocolate brown), and mode of solidification. Maximum temperatures at the sulfur cones at Volcan Azufre were between 155 and 235°C, although Colony and Nordlie (1973) consider the temperature of the molten sulfur to have been below 160°C based on their model of the mechanism of eruption which will be discussed below. For both areas the sulfur was apparently erupted below 160°C, the point at which the viscosity of the fluid increases from several centipoise to almost 1000 poise (Fig. 10). Thus, the viscosities of these flows increased from about 7 centipoise to 76 centipoise as the melt cooled. No natural terrestrial sulfur flow has been identified which was erupted above 200°C and which would have undergone a drastic decrease in viscosity between 160 and 180°C.

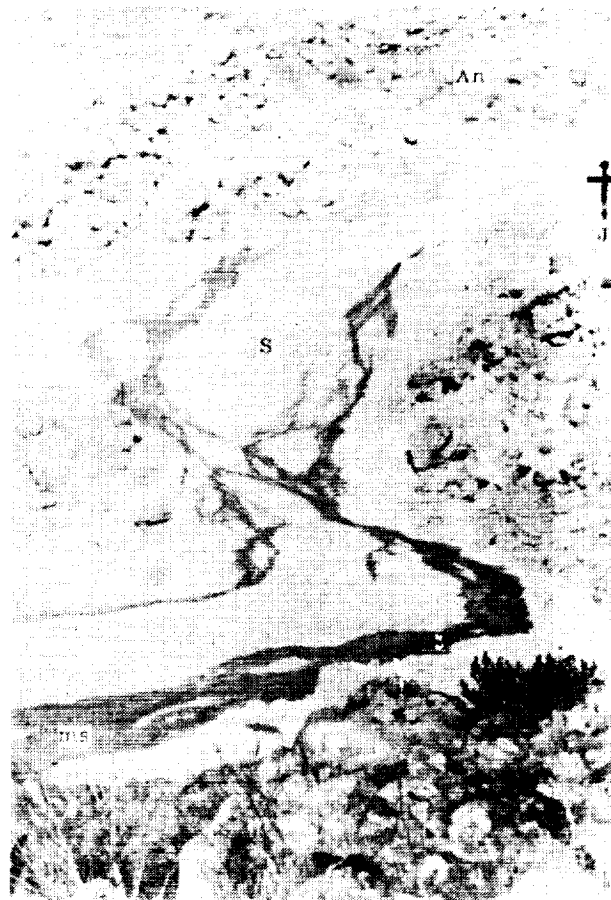


Figure 18. Molten sulfur flow (ms) from a small vent (J) in Sulphur Crater at Siretoko-Iōsan. The relatively smooth, light areas are older sulfur flows (S) and rough looking areas are the andesitic walls of the crater (An). (From Watanabe, 1940)

Flow Characteristics

The sulfur flows from the different areas exhibit a variety of surface textures and flow structures which suggest that liquid sulfur develops a chilled crust and behaves similarly to basaltic lava flows. Watanabe describes the flows in Japan as cooling more rapidly at the margins and at the surface such that the top moved more slowly than the interior. This resulted in a pahoehoe-like surface texture near the vent and tension cracks in the upper crust as it was rafted along by the fluid sulfur below (Fig. 19). After the end of an eruption the interior remained fluid for a short time.

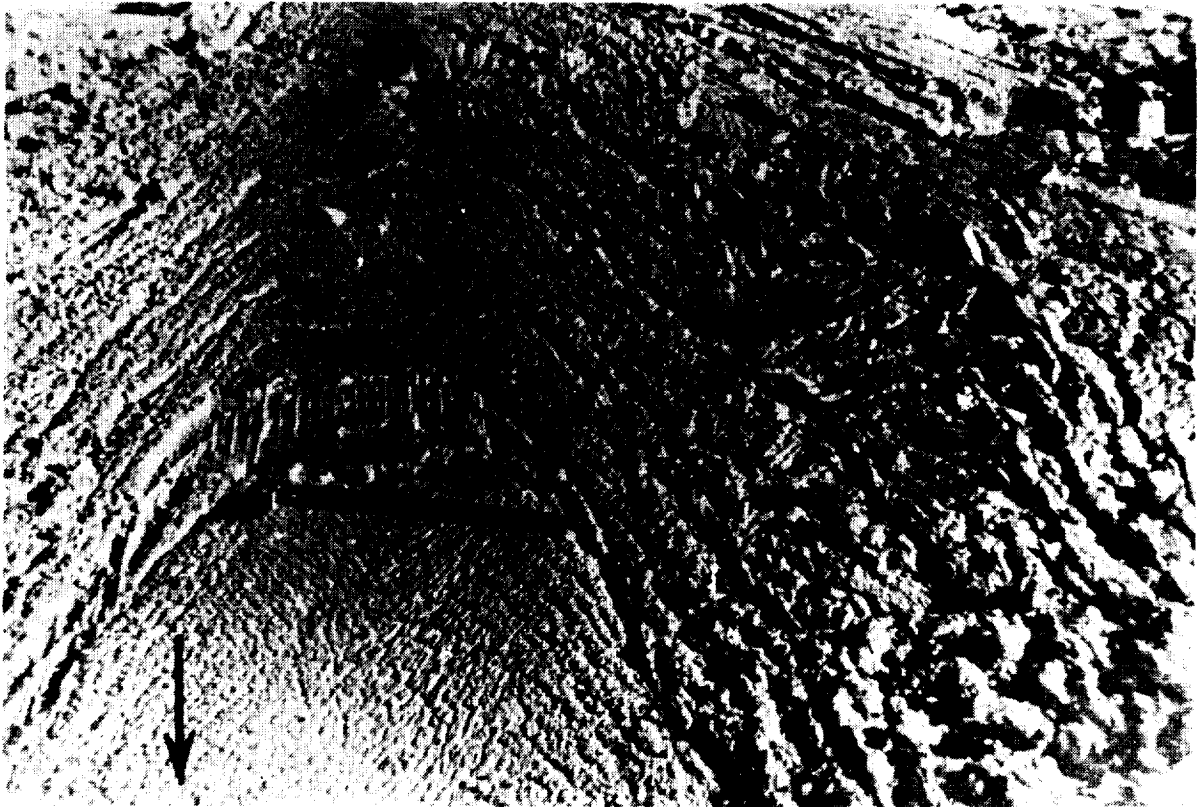


Figure 19. Upper chilled crust of a flow in Japan has been pulled apart by underlying flow to form tension cracks. Arrow shows flow direction. (From Watanabe, 1940)

Channels developed in the central parts of some flows (Fig. 20). At the distal ends of the flows Watanabe (1940) described an aa-like texture. He also mentions the sulfur flows forming miniature models of lava-falls, lava treemolds, and lava tubes. Sulfur stalactites and stalagmites formed near the vent (Fig. 21) and near the sulfur-falls. The sulfur flows typically formed many branches.

In the Galapagos Islands the flows spread out near the ends and formed several lobes similar to a birdfoot delta. Colony and Nordlie (1973) described concentric ridges oriented perpendicular to the flow direction (Fig. 22) which may be similar to pahoehoe surface texture but which they compare to ridges that are formed in confined channels during laminar flow. Both single and composite flows are present on Isabela Island.

Lobe-like forms and rivulets were described by Skinner (1970) on the surface of the flow in Hawaii. This surface texture was also described by Watanabe (1940) for the flows in Japan (Fig. 23) and appear to be small tube-fed toes. Skinner (1970) also described the base of the flow as penetrating into the loose scoria over which it passed. He considered the flow to have cooled as a single unit.

The sulfur flows in Hawaii (Skinner, 1970) and Japan (Watanabe, 1940) were relatively pure sulfur, whereas those in the Galapagos Islands ranged from 99% pure sulfur to more than 50% opalized basalt fragments. The altered fragments are similar in size and character to those in the material from which the flows erupted. Within some of the flows in Japan, small grains of bleached



Figure 20. Channel formed down the center of a narrow branch of a sulfur flow in Japan. This flow almost fills the entire photograph and the boundaries can be detected by albedo markings representing topography. Flow within the channel caused echelon cracks to form in the solidified crust along the flow margins. Arrow shows direction of flow. The rough surface, particularly to the right of the recent flow, is an older sulfur flow. (From Watanabe, 1940)

clayey rock were found but they were rare. Watanabe (1940) considered these grains to have originated from the walls of the sulfur reservoir and to be composed of kaolinite and opal formed by the alteration of andesite by acid solutions. Grain sizes of sulfur crystals within the flows were reported by Colony and Nordlie (1973) to have a maximum dimension of about 8 mm. Skinner (1970) observed a grain size variation of large crystals, with cleavage surfaces of about 1 cm^2 , in the interior of the flow and microscopic crystals at

the surface. This pattern of crystal size variations would indicate fast cooling of the surface layer, producing a chilled crust, which helped to insulate the interior of flow and allowed a slower rate of cooling to produce larger crystals.

The cooling process on the sulfur flows in Japan was accompanied by a color change from deep chocolate brown to a light brown of the chilled crust, a rigid sulfur glass. After a short time many small yellow crystals of rhombic sulfur (orthorhombic (α) sulfur in present nomenclature) began to form on the surface (Fig. 24), and within an hour the entire surface had crystallized. Some of the sulfur was vesicular and contained monoclinic (β) sulfur crystals in many of the vugs. The density of the Japanese flows ranged from 2.01 to 2.09 g/cm^3 .

Some of the earlier flows in Japan were a light green to yellowish green after crystallizing which probably indicates the presence of impurities. Spectroscopic analyses of several sulfur samples indicate that barium and copper were contained in all of the flows. Other impurities are given in Watanabe (1940).



Figure 21. Sulfur stalactites which formed near the sulfur vent in the explosion crater at Siretoko-Iôsan. A long-handled rock pick is standing in the shadow of the overhang. (From Watanabe, 1940)



Figure 22. Concentric ridges oriented perpendicular to flow direction formed in the lower parts of the lobate sulfur flows at Volcan Azufre, the Galapagos Islands. This particular flow was composed of 47% sulfur and 53% opalized basalt fragments. Rock hammer is shown for scale. (From Colony and Nordlie, 1973)

Mechanisms of Eruptions

Proposed mechanisms for the eruptions of the sulfur flows all involve remelting of fumarolic sulfur deposits but differ in the method by which the sulfur reaches the surface.

At Siretoko-Iôsan the sulfur eruptions occurred cyclically with acid water and gases which led Watanabe (1940) to propose a very specialized geyser system in which a near surface chamber is filled with sulfur and meteoric water. The sulfur that migrated to the chamber was remelted by a rise in the local heat gradient. Sulfur filled part of the chamber and moved up the conduit where it cooled

and formed a plug blocking the rise of the sulfur. As the water in the chamber was heated it turned to steam and the pressure within the chamber rose until it overcame the strength of the plug and the eruption of material began. The sulfur was extruded first, followed by water, and then by steam (Fig. 25). After the chamber was empty, the process was repeated. One of the major assumptions of this mechanism is that the conduit joins the lower part of the chamber and not the upper so that the sulfur is able to block it. This mechanism explains the cyclic activity and the presence of definable vents.

On Isabela Island and probably on Hawaii the method of eruption is not as complex.



Figure 23. Toe-like features on a sulfur flow in Japan. Note the central curvilinear collapse features on most of the toes, which suggest that flow occurred through tubes. Also note the otherwise smooth surface. (From Watanabe, 1940)

Sulfur is deposited near and on the surface by fumarolic activity, resulting in an equilibrium system if no new sulfur is added to the system and the thermal gradient remains constant. Newly deposited sulfur continuously buries older sulfur. The buried sulfur eventually reaches a level at which the subsurface temperature is great enough to remelt it. The melted sulfur is then carried back to the surface by the rising gases. If, however, the local thermal gradient rises, more sulfur is melted than is replaced. This remelted sulfur may saturate the rock and flow laterally or downgradient, where it may then reach the surface downslope and form a surface flow. Because the sulfur must flow through the porous material by this mechanism, the sulfur must have been below 160°C in temperature which is below the high viscosity jump. This method explains the lack of a definable

vent and the entrained particles of opalized basalt within some of the flows. The mechanism of eruption in Hawaii may have been similar to the one in the Galapagos Islands. The local heating in Hawaii may have been initiated by the 1950 eruption of Mauna Loa.

4.2 MAN-MADE SULFUR FLOWS

Additional information about the behavior of molten sulfur can be obtained from the sulfur industry. Sulfur associated with limestone or salt domes is mined in the United States by the Frasch process in which sulfur is melted at depth, brought to the surface, and cooled in large vats. The Frasch process, first used economically in 1903, consists of three pipes inserted concentrically into a drill hole and perforated at different levels (Fig.

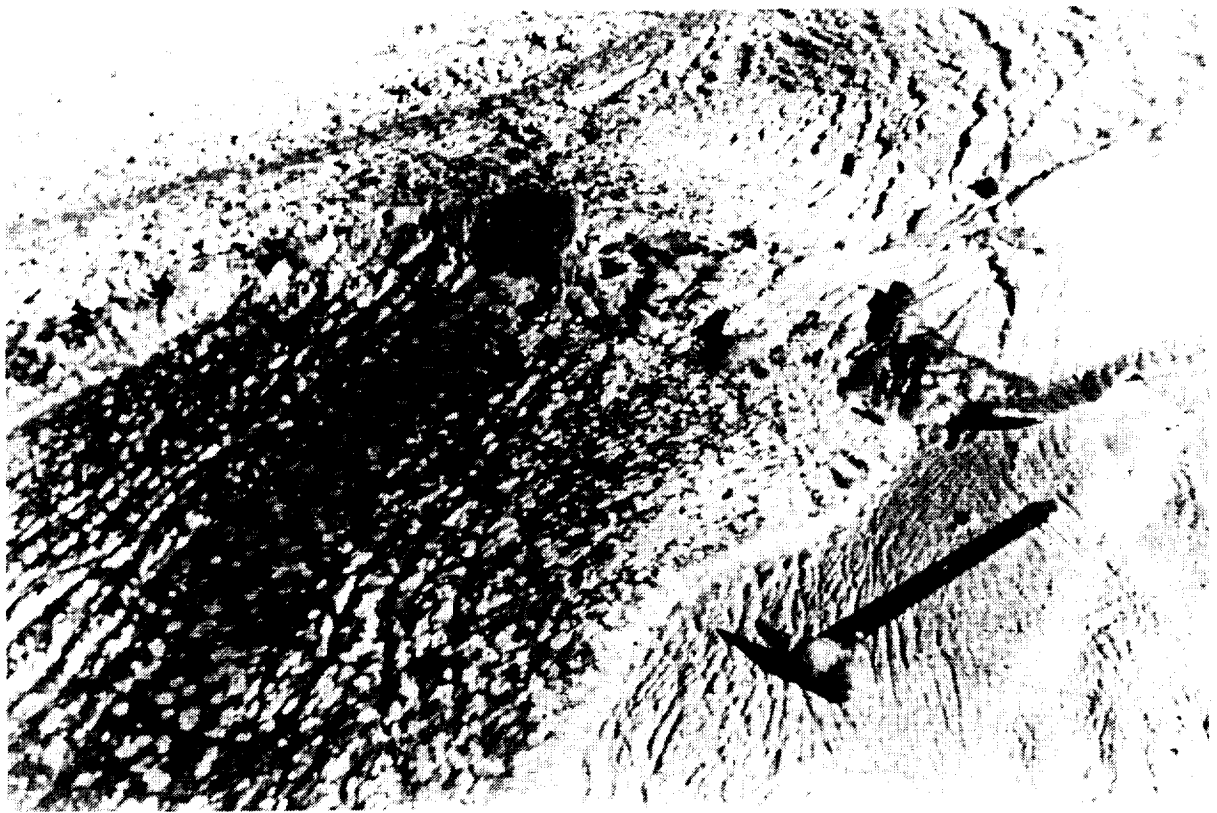


Figure 24. The mottled appearance of a sulfur flow shortly after eruption. Light areas within the darker material are points of crystallization in the upper rigid sulfur glass. Within an hour after crystallization began, the entire surface was yellow. Also of interest are the ridges on the surface 'downstream' of a large rafted section tilted into the flow. These features are similar to pahoehoe flows. Tension cracks have formed 'upstream' of the obstacle. Flow was toward the lower lefthand corner. (From Watanabe, 1940)

26). The perforated sections are kept separated from each other by rings. Hot water at about 165°C (330°F; Shearon and Pollard, 1950) is injected into the sulfur deposit, melting the sulfur within an inverted cone-shaped area with the apex at the base of the well. The liquid sulfur migrates downward and collects at the base of the well. If the well is open to the atmosphere, the sulfur will eventually rise about halfway up the pipe under hydrostatic pressure. Air is then entrained into the sulfur causing it to rise to the surface. The air is removed from the sulfur at a relay station, a separator, or as it is discharged into a vat. As the sulfur is pumped into a storage vat it forms thin flows similar to natural sulfur flows and which may be use-

ful analogs. An extensive discussion of sulfur mining is offered by Shearon and Pollard (1950).

Most cooling vats are about 100 m long and wide and consist of a layered sequence of sulfur flows. The sulfur is pumped into a vat at about 14 tons/minute at a temperature of about 138°C until most of the surface is covered by a 5 to 8 cm layer of sulfur which cools in about 8 hours. Thin layers of sulfur in the vat are preferred because of the danger of developing pockets of molten sulfur. The high insulating properties of sulfur will allow hot pockets to remain for 6 to 8 months if overlaid by a meter or so of solidified sulfur, and some have been known to exist for 4 to

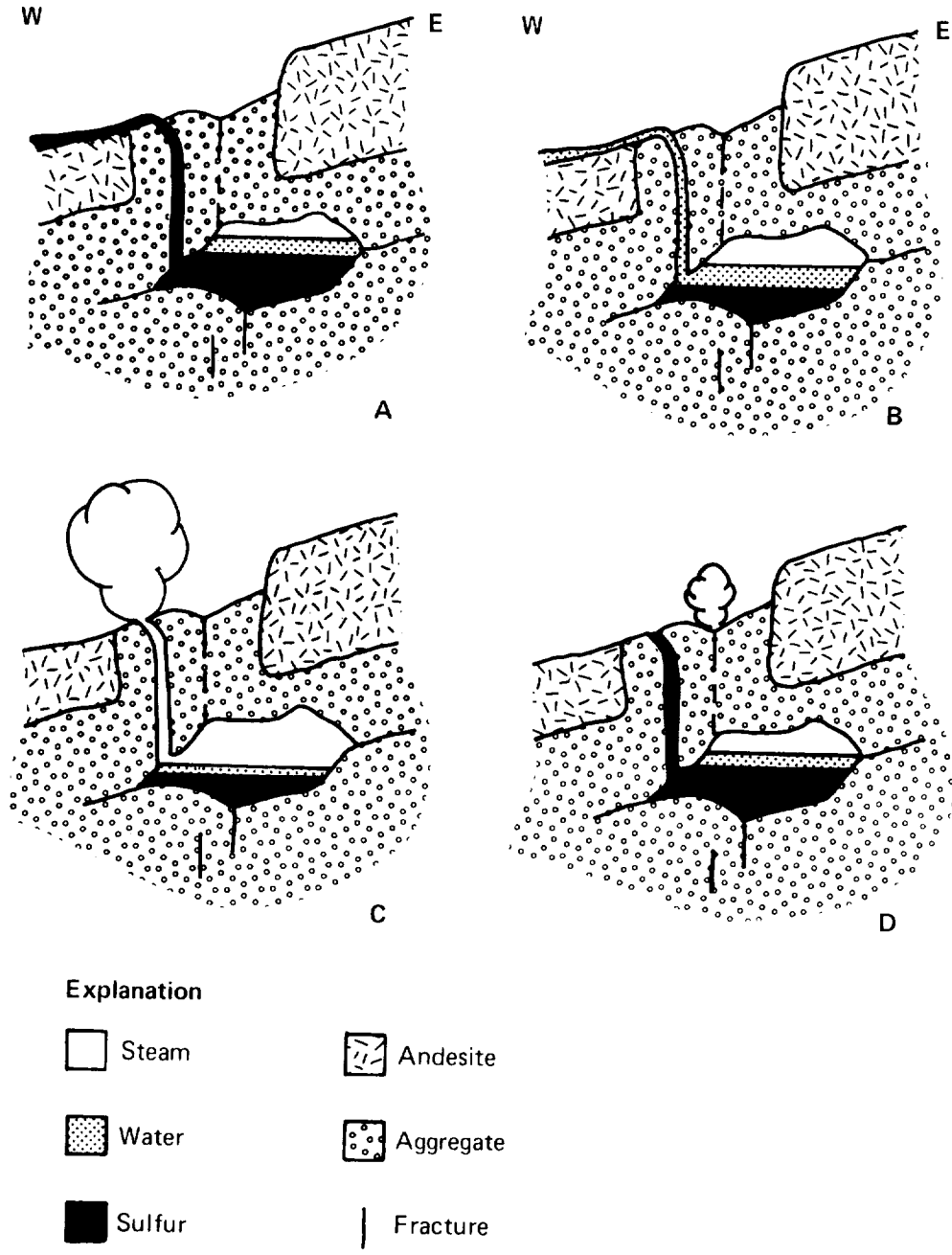


Figure 25. Schematic diagram of the mechanism of sulfur eruptions at Sulphur Crater, Japan. A) Pressure in a subsurface chamber filled with water and sulfur becomes great enough by the formation of steam to force the sulfur upward through a conduit to erupt onto the surface. B) Sulfur is depleted within the chamber so that it falls below the level of the conduit and hot water is then forced to the surface. C) After the water level also drops below that of the conduit, steam erupts from the vent. D) Pressure is relieved within the chamber and the process repeats itself. Hot sulfur and water migrate through the aggregate and fill the chamber and steam begins to form, some of which moves to the surface through fractures. As the pressure builds, sulfur is forced to the surface where it forms a cooled plug blocking the conduit. Eruptions begin when the pressure within the chamber can overcome the plug. (Modified after Watanabe, 1940)

5 years (per comm., Gray, Duval Corporation, Galveston, Texas). The sulfur flows in the vat follow the underlying topography and spread out laterally over most of the area. Parts of the surface that are not covered are similar to kipukas. Similar 'holes' in the flow, but on a smaller scale, are found near the edges and are apparently formed by the coalescing of 2 flow lobes. The edges are lobate on both a large and small scale, and in some areas overlapping toes of sulfur occur.

Surface textures vary across the surface of a single flow unit and can be divided into two types: smooth and irregular. In several areas the smooth surface is prominent near the end of the flow and the irregular or hummocky texture dominates closer to the source. The reason for the apparent reversal in texture from that associated with lava flows is undetermined. Tension cracks or joints are prevalent across the vat surface. New flows cover some of the joints; however, in many cases the joints cut both old and new flows, which may indicate that the joints propagate upwards through the more recent material.

At the point where sulfur is added to the vat, a turbulent pool is formed by the incoming sulfur and by melting of the underlying sulfur. Raised 'levees' mark the extent of the pool and probably formed by continual splashing of the sulfur around the edges. These raised edges are higher near the source and tend to overhang slightly the surface of the pool which is very smooth after solidification. In some areas the pool has apparently thermally undercut the sides so that after the material has cooled, thin overhangs extend out over the pools of sulfur. Beyond the pool, 'downstream' from the source, the surface of the flow is extremely rough and forms irregular arcuate ridges. Beneath the source pipe for

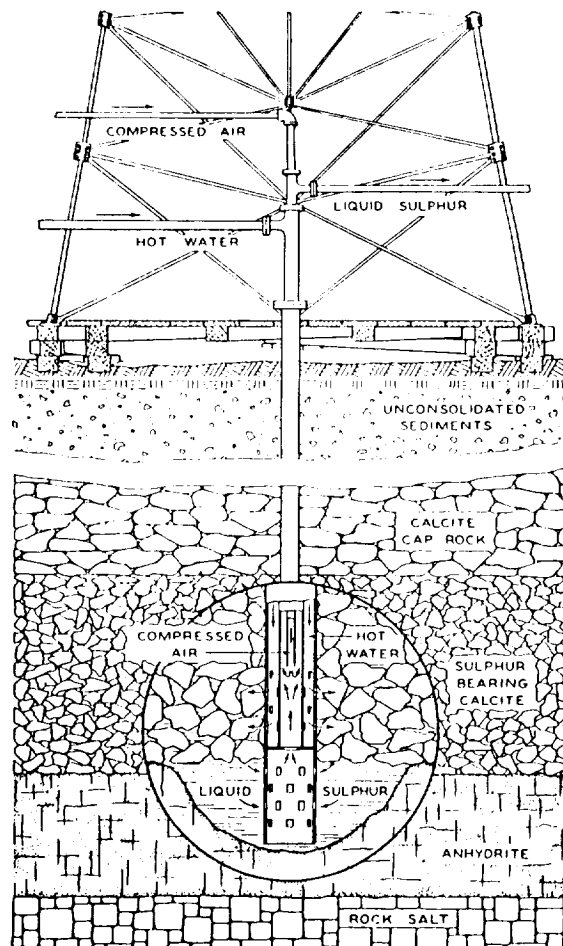


Figure 26. Schematic diagram of the Frasch mining process. Pipe and perforation arrangement at the base of the hole is shown in the enlargement. Hot water is pumped down the outermost pipe and released into the sulfur deposits. The sulfur melts, migrates downward to the base of the well, then rises up the center pipe to a point where it is mixed with compressed air and forced to the surface. Cooling vats can be located adjacent to the well site, or the sulfur can be shipped molten and cooled at other facilities. (From Texas Gulf Sulphur Company, 1953)

the sulfur a conical construct is built from a combination of splashing within the pool and sulfur falling from the pipe and dribbling down the sides.

5. SUMMARY

Sulfur is an incredibly complex element whose chemistry, occurrence, and properties are not completely understood. Intramolecular allotropes which are important to the study of volcanism on Io include ring molecules which can be isolated as solids, large chains or polymers occurring in both liquids and solids, and small molecules. The most common form of solid sulfur is orthorhombic (α) sulfur. Other forms which are considered unstable under terrestrial conditions but which may be stable under ionian conditions are polymeric sulfur, cyclohepta sulfur (S_7), monoclinic (γ) sulfur, cyclodeca sulfur (S_{10}), and possibly cyclooctadeca sulfur (S_{18}). Solid sulfur formed by quenching a melt is determined by the thermal history of the material and, therefore, the composition of the liquid. The important molecular species within liquid sulfur change in concentration with temperature and consist of cyclo- S_8 , polymeric chains, and small molecules of S_3 , S_4 , and S_5 . The concentrations of these groups control the physical properties of the melt and the crystallized solid. Polymerization of liquid sulfur causes discontinuities in viscosity, density, thermal conductivity, and specific heat. Changes in viscosity from several centipoise to almost a thousand poise would have a large effect on flow features and texture. The color of liquid sulfur and solid sulfur formed by quenching is also very important. Color changes within a melt form a spectrum from bright, clear yellow at the melting point to dark, opaque red at the boiling point. The red is largely attributed to S_3 , S_4 , and S_5 . The color of quenched sulfur depends on its thermal history.

Terrestrial sulfur flows, both natural and man-made, apparently behave similarly to

silicate flows. Natural sulfur flows are rare but have been found in Japan, the Galapagos Islands, and Hawaii. These flows are considered to have formed by melting and mobilization of fumarolic deposits, and only the flows in Japan apparently issued from a defined vent. The temperatures at which the sulfur flows were erupted are considered to be below 160°C so that the flows must have been extremely fluid (7 to 76 centipoise viscosity). The flows are relatively thin but still possess a chilled crust as evidenced by: 1) ridges and fractures formed in a rigid or semi-rigid upper layer pulled along by underlying molten sulfur; 2) a microcrystalline surface layer over a coarsely crystalline interior; and 3) lobe-like forms and rivulets which appear to be formed by tube flows. For further study of flowing sulfur, the man-made flows from the Frasch mining process may be useful analogs, as natural flows are rare.

Important aspects of ionian volcanism are the color and morphology of the flows. The colors tend to follow those of sulfur quenched or cooled from different temperatures or at different cooling rates. Variation in morphology of the flows from short narrow flows to broad sheets could be explained by different viscosities, as exhibited by sulfur. However, for this to occur only the upper layer could be quenched allowing the interior to cool slowly and to experience the changes in viscosity as it cooled. More work is needed to define the exact chemistry, properties and behavior of sulfur under ionian conditions so that more precise models could be derived to predict the processes of sulfur volcanism on Io.

REFERENCES

- Bacon, R.F., and Fanelli, J., 1943. The viscosity of sulfur, *J. Am. Chem. Soc.*, *65*, 639-648.
- Banfield, A.F., 1954. Volcanic deposits of elemental sulfur, *Canadian Mining and Metallurgical Bull.*, *47*, 769-775.
- Carr, M.H., Masursky, H., Strom, R.G., and Terrile, R.J., 1979. Volcanic features of Io, *Nature*, *280*, 729-733.
- Clark, S.P., Jr., 1966. Viscosity, in Clark, S.P., Jr., ed., *Handbook of Physical Constants*, U.S. Geol. Surv., Memoir 97, 291-300.
- Colony, W.E., and Nordlie, B.E., 1973. Liquid sulfur at Volcan Azufre, Galapagos Islands, *Economic Geology*, *68*, 371-380.
- Dale, J.M., and Ludwig, A.C., 1965. Mechanical properties of sulfur, in Meyer, B., ed., *Elemental sulfur, chemistry and physics*: Interscience Publishers, New York, 161-178.
- Donohue, J., 1965. The structures of the allotropes of solid sulfur, in Meyer, B., ed., *Elemental sulfur, chemistry and physics*: Interscience Publishers, New York, 13-43.
- Donohue, J., 1974. *The structures of the elements*: Wiley-Interscience, New York, 325-369.
- Donohue, J., and Meyer, B., 1965. The naming of sulfur allotropes, in Meyer, B., ed., *Elemental sulfur, chemistry and physics*: Interscience Publishers, New York, 1-11.
- Fanale, F.P., Johnson, T.V., and Matson, D.L., 1974. Io: A surface evaporite deposit?, *Science*, *186*, 922-925.
- Fanale, F.P., Brown, R.H., Cruikshank, D.P., and Clark, R.N., 1979. Significance of absorption features in Io's IR reflectance spectrum, *Nature*, *280*, 761-763.
- Johnson, T.V., Cook, A.F., II, Sagan, C., and Soderblom, L.A., 1979. Volcanic resurfacing rates and implications for volatiles on Io, *Nature*, *280*, 746-750.
- MacKnight, W.J., and Tobolsky, A.V., 1965. Properties of polymeric sulfur, in Meyer, B., ed., *Elemental sulfur, chemistry and physics*: Interscience Publishers, New York, 95-107.
- Meyer, B., 1965. Preparation and properties of sulfur allotropes, in Meyer, B., ed., *Elemental sulfur, chemistry and physics*: Interscience Publishers, New York, 45-69.
- Meyer, B., 1968. Elemental sulphur, in Nickless, G., ed., *Inorganic sulphur chemistry*: Elsevier Publishing Company, Amsterdam, 241-258.
- Meyer, B., 1976. Elemental sulfur, *Chemical Reviews*, *76*, 367-388.
- Meyer, B., 1977. *Sulfur, energy, and environment*: Elsevier Scientific Publishing Company, Amsterdam, 488 p.
- Meyer, B., Oommen, T.V., and Jensen, D., 1971. The color of liquid sulfur, *J. Phys. Chem.*, *75*, 912-917.
- Morabito, L.A., Synnott, S.P., Kupferman, P.N., and Collins, S.A., 1979. Discovery of currently active extraterrestrial volcanism, *Science*, *204*, 972.
- Murase, T., and McBirney, A.R., 1970. Viscosity of lunar lavas, *Science*, *167*, 1491-1493.
- Nash, D.B., and Fanale, F.P., 1977. Io's surface composition based on reflectance spectra of sulfur/salt mixtures and proton-irradiation experiments, *Icarus*, *31*, 40-80.
- Nelson, R.M., and Hapke, B.W., 1978. Spectral reflectivities of the Galilean satellites and Titan, 0.32 to 0.86 micrometers, *Icarus*, *36*, 304-329.
- Sagan, C., 1979. Sulphur flows on Io, *Nature*, *280*, 750-753.
- Shearon, W.H., Jr., and Pollard, J.H., 1950. Modern sulfur mining, A staff-industry collaborative report..., *Industrial and Engineering Chemistry*, *42*, 2188-2198.
- Skinner, B.J., 1970. A sulfur lava flow on Mauna Loa, *Pacific Science*, *24*, 144-145.
- Smith, B.A., Soderblom, L.A., Johnson, T.V., Ingersoll, A.P., Collins, S.A., Shoemaker, E.M., Hunt, G.E., Masursky, H., Carr, M.H., Davies, M.E., Cook, A.F., II, Boyce, J., Danielson, G.E., Owen, T., Sagan, C., Beebe, R.F., Veverka, J., Strom, R.G., McCauley, J.F., Morrison, D., Briggs, G.A., and Suomi, V.E., 1979a. The Jupiter system through the eyes of Voyager I, *Science*, *204*, 951-971.
- Smith, B.A., Shoemaker, E.M., Kieffer, S.W., and Cook, A.F., II, 1979b. The role of SO₂ in volcanism on Io, *Nature*, *280*, 738-743.
- Texas Gulf Sulphur Company, 1953. *Facts about sulphur*, Texas Gulf Sulphur Co., New York, 52 p.

- Thackray, M., 1970. Melting point intervals of sulfur allotropes, *J. Chem. Eng. Data*, 15., 495-497.
- Tuller, W.N., ed., 1954. *The sulphur data book*: McGraw-Hill Book Co., Inc., New York, 143 p.
- Wamsteker, W., Kroes, R.L., and Fountain, J.A., 1974. On the surface composition of Io, *Icarus*, 23, 417-424.
- Watanabe, T., 1940. Eruptions of molten sulphur from the Siretoko-Iôsan Volcano, Hokkaidô, Japan, *Japanese Jour. of Geology and Geography*, 17, 289-310.

1. Report No. NASA CR-3594		2. Government Accession No.		3. Recipient's Catalog No.	
4. Title and Subtitle A PRIMER ON SULFUR FOR THE PLANETARY GEOLOGIST				5. Report Date September 1982	
				6. Performing Organization Code EL-4	
7. Author(s) Eilene Theilig				8. Performing Organization Report No.	
9. Performing Organization Name and Address Planetary Geology Group Department of Geology Arizona State University Tempe, AZ 85287				10. Work Unit No.	
				11. Contract or Grant No. NAGW-132	
				13. Type of Report and Period Covered Contractor Report	
12. Sponsoring Agency Name and Address Office of Space Science and Applications National Aeronautics and Space Administration Washington, DC 20546				14. Sponsoring Agency Code	
15. Supplementary Notes NASA Technical Monitor: Joseph M. Boyce Summary Report					
16. Abstract <p>Sulfur has been proposed as the dominant composition for the volcanic material on Io. Sulfur is a complex element which forms many intramolecular and intermolecular allotropes exhibiting a variety of physical properties. Cyclo-S₈ sulfur is the most abundant and stable molecular form. The important molecular species within liquid sulfur change in concentration with temperature and consist of cyclo-S₈, polymeric chains, and small molecules as S₃, S₄, and S₅. Concentrations of the allotropes control the physical properties of the melt. Discontinuities in density, viscosity, and thermal properties reflect the polymerization process within liquid sulfur. Increasing concentrations of S₃, S₄, and S₅ with temperature cause the color change from yellow to red. Variations in the melting point are related to autodissociation of the liquid. Many solid forms of sulfur have been identified but only orthorhombic α and monoclinic β sulfur, both composed of cyclo-S₈ sulfur, are stable under terrestrial conditions. Other solid allotropes are composed of various molecular species and may be formed through reactions of sulfur compounds or by quenching the melt. Physical properties of solid sulfur are dependent on the allotrope and, in some cases, the thermal history. Although only two solid allotropes are considered stable, others may be important on Io.</p> <p>Natural terrestrial sulfur flows have been identified in several areas, three of which are described here: 1) Siretoko-Iōsan, Japan; 2) Volcan Azufre, Galapagos Islands; and 3) Mauna Loa, Hawaii. All of the flows are associated with fumarolic areas and are considered to have formed by the melting and mobilization of sulfur deposits. Only the flows in Japan apparently issued from a definable vent, whereas in Volcan Azufre the flows headed in talus deposits; in Hawaii, the head of the flow was apparently covered by talus. Surface textures of the flows indicate a behavior of molten sulfur similar to that of silicate lava. Tension cracks in the top layer, pahoehoe-like surface texture, and a microcrystalline surface layer and coarsely crystalline interior all suggest the formation of a chilled crust. Channels, rivulets, and lobate edges were also described for the flows. Temperature at which sulfur was erupted was not measured for any of the flows but for various reasons none of them were considered to have erupted above 160°C.</p> <p>Man-made sulfur flows may be formed as part of the Frasch mining process by which sulfur is removed from the sub-surface in a liquid state. For storage purposes the molten sulfur may be pumped into large vats to solidify. As the sulfur is pumped into the vat, it forms a thin flow exhibiting smooth and irregular textures and lobate edges on both a large and small scale. Further studies of these flows could yield more information of the behavior of flowing sulfur.</p>					
17. Key Words (Suggested by Author(s)) Solar System Evolution Comparative Planetology Geologic Processes Volcanism Sulfur			18. Distribution Statement Unclassified - Unlimited Category 25		
19. Security Classif. (of this report) Unclassified		20. Security Classif. (of this page) Unclassified		21. No. of Pages 34	22. Price A03